

Entanglement and conservation of orbital angular momentum in spontaneous parametric down-conversion

S. P. Walborn, A. N. de Oliveira, R. S. Thebaldi, and C. H. Monken*

Universidade Federal de Minas Gerais, Caixa Postal 702, Belo Horizonte, MG 30123-970, Brazil

(Received 19 November 2003; published 25 February 2004)

We show that the transfer of the plane-wave spectrum of the pump beam to the fourth-order transverse spatial correlation function of the two-photon field generated by spontaneous parametric down-conversion leads to the conservation and entanglement of orbital angular momentum of light. By means of a simple experimental setup based on fourth-order (or two-photon) interferometry, we show that our theoretical model provides a good description for down-converted fields carrying orbital angular momentum.

DOI: 10.1103/PhysRevA.69.023811

PACS number(s): 42.50.St, 03.65.Ud, 42.50.Ar

I. INTRODUCTION

It is well established that when the paraxial approximation is valid, any electromagnetic beam with an azimuthal phase dependence of the form $e^{il\phi}$ carries an orbital angular momentum $l\hbar$ per photon [1]. Interesting enough by itself, due to its fundamental character, this fact also raises possibilities for technical applications. For example, in the rapidly developing field of quantum information, it has been pointed out recently that it is possible to increase the amount of information carried by a single photon by encoding qubits in the orbital angular momentum [2,3]. Laguerre-Gaussian (LG) beams are the most known and studied examples of beams carrying orbital angular momentum. Devices that discriminate the orbital angular momentum of Laguerre-Gaussian beams have been reported and experimentally tested for very low intensities, suggesting that they should work at the single-photon level [4].

An important potential application of light beams carrying orbital angular momentum is the generation of photon pairs with discrete multidimensional entanglement [5]. This can be obtained by means of spontaneous parametric down-conversion (SPDC) pumped by a LG beam. Denoting by $|m\rangle$ a one-photon state carrying an orbital angular momentum $m\hbar$ and by l the azimuthal index of the LG pump beam, the two-photon state generated by SPDC can be written as

$$|\psi\rangle = \sum_{m=-\infty}^{+\infty} C_m |l-m\rangle |m\rangle. \quad (1)$$

This expression is based on the hypothesis that orbital angular momentum is conserved in SPDC. Some authors have studied this issue [2,6–8], and experimental results [5] suggest that orbital angular momentum is in fact conserved. One has to consider, however, that although the process of down-conversion itself may conserve angular momentum, in most cases, the pump beam propagates in a birefringent nonlinear crystal as an extraordinary beam. The anisotropy of the medium causes a small astigmatism in the LG beam as it propagates, breaking its circular symmetry in the transverse plane.

This symmetry breaking is equivalent to an exchange of angular momentum between the medium and pump beam, so that conservation holds only on average. This effect depends on both the angular momentum of the pump beam and the crystal length, being negligible for thin crystals and low values of l . A detailed account of this problem will be published elsewhere.

In an earlier paper [9], we showed that the phase matching conditions in SPDC are responsible for a transfer of the amplitude and phase characteristics of the pump beam to the two-photon field. In fact, it is the plane-wave spectrum or the so-called angular spectrum of the pump beam that is transferred to the fourth-order spatial correlation properties of the down-converted field. In this work, we demonstrate theoretically and experimentally that the conservation of orbital angular momentum as well as the multidimensional entanglement in the SPDC process in the thin crystal paraxial approximation is a direct consequence of the transfer of the plane-wave spectrum from the pump beam to the two-photon state. By means of a simple experimental setup based on fourth-order (or two-photon) interferometry, we show that our theoretical model provides a good description for down-converted fields carrying orbital angular momentum.

II. THEORY

A. State generated by SPDC

In the monochromatic and paraxial approximations, the state generated by noncollinear SPDC can be written as [9,10]

$$|\text{SPDC}\rangle = C_1 |\text{vac}\rangle + C_2 |\psi\rangle, \quad (2)$$

where

$$|\psi\rangle = \sum_{\sigma_s, \sigma_i} C_{\sigma_s, \sigma_i} \int \int_D d\mathbf{q}_s d\mathbf{q}_i \Phi(\mathbf{q}_s, \mathbf{q}_i) |\mathbf{q}_s, \sigma_s\rangle_s |\mathbf{q}_i, \sigma_i\rangle_i. \quad (3)$$

The coefficients C_1 and C_2 are such that $|C_2| \ll |C_1|$. Here C_2 depends on the crystal length, the nonlinearity coefficient, and the magnitude of the pump field, among other factors. The kets $|\mathbf{q}_j, \sigma_j\rangle$ represent one-photon states in plane-wave modes labeled by the transverse component \mathbf{q}_j of the wave

*Electronic address: monken@fisica.ufmg.br

vector \mathbf{k}_j and by the polarization σ_j of the mode $j=s$ or i . The polarization state of the down-converted photon pair is defined by the coefficients C_{σ_s, σ_i} . The function $\Phi(\mathbf{q}_s, \mathbf{q}_i)$ is given by [9]

$$\Phi(\mathbf{q}_s, \mathbf{q}_i) = \frac{1}{\pi} \sqrt{\frac{2L}{K}} v(\mathbf{q}_s + \mathbf{q}_i) \text{sinc}\left(\frac{L|\mathbf{q}_s - \mathbf{q}_i|^2}{4K}\right), \quad (4)$$

where $v(\mathbf{q})$ is the normalized angular spectrum of the pump beam, L is the length of the nonlinear crystal in the propagation (z) direction, and K is the magnitude of the pump field wave vector. The integration domain D is, in principle, defined by the conditions $q_s^2 \leq k_s^2$ and $q_i^2 \leq k_i^2$. However, in most experimental conditions, the domain in which $\Phi(\mathbf{q}_s, \mathbf{q}_i)$ is appreciable is much smaller. If the crystal is thin enough, the sinc function in Eq. (4) can be approximated by 1. We assume that $\Phi(\mathbf{q}_s, \mathbf{q}_i)$ does not depend on the polarizations of the down-converted photons. In some cases, this is not true, especially when one is dealing with type-II phase matching, in which case the two photons have orthogonal polarizations. However, this dependence can be made negligible by the use of compensators in the down-converted beams [11].

The two-photon detection amplitude, which can be regarded as a photonic wave function, is

$$\Psi(\mathbf{r}_s, \mathbf{r}_i) = \langle \text{vac} | \mathbf{E}_i^{(+)}(\mathbf{r}_i) \mathbf{E}_s^{(+)}(\mathbf{r}_s) | \psi \rangle, \quad (5)$$

where $\mathbf{E}_j^{(+)}(\mathbf{r})$ is the field operator for the plane-wave mode j . In the paraxial approximation, $\mathbf{E}_j^{(+)}(\mathbf{r})$ is

$$\mathbf{E}_j^{(+)}(\mathbf{r}) = e^{ikz} \sum_{\sigma} \int d\mathbf{q} \mathbf{a}_j(\mathbf{q}, \sigma) \boldsymbol{\epsilon}_{\sigma} e^{i[\mathbf{q} \cdot \boldsymbol{\rho} - (q^2/2k)z]}. \quad (6)$$

The operator $\mathbf{a}_j(\mathbf{q}, \sigma)$ annihilates a photon in mode j with transverse wave vector \mathbf{q} and polarization σ .

In the analysis that follows, we do not need to consider polarization. So $\Psi(\mathbf{r}_s, \mathbf{r}_i)$ will be treated as a scalar function. In addition, we will work in the far field and make the following simplifications: $z_s = z_i = Z$, $k_s = k_i = \frac{1}{2}K$. It is known that if the paraxial approximation is valid, the two-photon wave function is

$$\Psi(\boldsymbol{\rho}_s, \boldsymbol{\rho}_i, z_s, z_i) = \mathcal{E}\left(\frac{\boldsymbol{\rho}_s + \boldsymbol{\rho}_i}{2}, Z\right) \mathcal{F}\left(\frac{\boldsymbol{\rho}_s - \boldsymbol{\rho}_i}{\sqrt{2}}, Z\right), \quad (7)$$

where $\mathcal{E}(\boldsymbol{\rho}, z)$ is the normalized electric field amplitude of the pump beam and

$$\mathcal{F}(\boldsymbol{\rho}, z) = \frac{\sqrt{KL}}{2\pi z} \text{sinc}\left(\frac{KL}{8z^2} \boldsymbol{\rho}^2\right).$$

In order to clean up the notation, we will omit the dependence on the z coordinate hereafter. We see that the two-photon wave function Ψ carries the same functional form as the pump beam amplitude, calculated in the coordinate $\boldsymbol{\rho} = \frac{1}{2}\boldsymbol{\rho}_s + \frac{1}{2}\boldsymbol{\rho}_i$. The pump beam field $\mathcal{E}(\boldsymbol{\rho})$ is characterized by its wavelength λ_0 and its waist w_0 . To be more precise, we

will write \mathcal{E} as $\mathcal{E}(\boldsymbol{\rho}; \lambda_0, w_0)$. Since we are working with down-converted fields satisfying $\lambda_s = \lambda_i = 2\lambda_0$, it is convenient to write Ψ in terms of a beam with the same angular spectrum of the pump field, as required by Eq. (7), but with a wavelength $\lambda_c = 2\lambda_0$ and a waist $w_c = \sqrt{2}w_0$. From the general form of Gaussian beams, apart from a phase factor and normalization constants, it is evident that

$$\mathcal{E}(\boldsymbol{\rho}; \lambda_0, w_0) = \mathcal{E}(\sqrt{2}\boldsymbol{\rho}; 2\lambda_0, \sqrt{2}w_0) \equiv \mathcal{U}(\sqrt{2}\boldsymbol{\rho}). \quad (8)$$

So Ψ can be put in the more convenient form

$$\Psi(\boldsymbol{\rho}_s, \boldsymbol{\rho}_i) = \mathcal{U}\left(\frac{\boldsymbol{\rho}_s + \boldsymbol{\rho}_i}{\sqrt{2}}\right) \mathcal{F}\left(\frac{\boldsymbol{\rho}_s - \boldsymbol{\rho}_i}{\sqrt{2}}\right). \quad (9)$$

Let us now suppose that the down-converter is pumped by a LG beam whose orbital angular momentum is $l\hbar$ per photon, described by the amplitude $\mathcal{E}_p^{l_i}(\boldsymbol{\rho}; \lambda_0, w_0)$. Here, p is the radial index. In order to study the conservation of angular momentum in SPDC, we will expand the two-photon wave function $\Psi(\boldsymbol{\rho}_s, \boldsymbol{\rho}_i)$ in terms of the LG basis functions $\mathcal{U}_{p_s}^{l_s}(\boldsymbol{\rho}_s) \mathcal{U}_{p_i}^{l_i}(\boldsymbol{\rho}_i)$: that is,

$$\Psi(\boldsymbol{\rho}_s, \boldsymbol{\rho}_i) = \sum_{l_s, p_s} \sum_{l_i, p_i} C_{p_s p_i}^{l_s l_i} \mathcal{U}_{p_s}^{l_s}(\boldsymbol{\rho}_s) \mathcal{U}_{p_i}^{l_i}(\boldsymbol{\rho}_i). \quad (10)$$

From the orthogonality of the LG basis, $C_{p_s p_i}^{l_s l_i}$ is given by

$$\begin{aligned} C_{p_s p_i}^{l_s l_i} &= \int \int d\boldsymbol{\rho}_s d\boldsymbol{\rho}_i \mathcal{U}_p^l\left(\frac{\boldsymbol{\rho}_s + \boldsymbol{\rho}_i}{\sqrt{2}}\right) \mathcal{F}\left(\frac{\boldsymbol{\rho}_s - \boldsymbol{\rho}_i}{\sqrt{2}}\right) \mathcal{U}_{p_s}^{*l_s}(\boldsymbol{\rho}_s) \mathcal{U}_{p_i}^{*l_i}(\boldsymbol{\rho}_i). \end{aligned} \quad (11)$$

Let us make the following coordinate transformation in Eq. (11): $\mathbf{R} = \boldsymbol{\rho}_s + \boldsymbol{\rho}_i$ and $\mathbf{S} = \frac{1}{2}(\boldsymbol{\rho}_s - \boldsymbol{\rho}_i)$. So

$$\begin{aligned} C_{p_s p_i}^{l_s l_i} &= \int \int d\mathbf{R} d\mathbf{S} \mathcal{U}_p^l\left(\frac{\mathbf{R}}{\sqrt{2}}\right) \mathcal{F}(\sqrt{2}\mathbf{S}) \mathcal{U}_{p_s}^{*l_s}\left(\frac{\mathbf{R}}{2} + \mathbf{S}\right) \\ &\quad \times \mathcal{U}_{p_i}^{*l_i}\left(\frac{\mathbf{R}}{2} - \mathbf{S}\right). \end{aligned} \quad (12)$$

When L is small enough (the thin-crystal approximation), \mathcal{F} can be approximated by 1 in Eq. (12), provided the order of the LG modes ($N = 2p + |l|$) is not too large. In this case, the integral in \mathbf{S} is proportional to $\mathcal{U}_{p_s}^{*l_s}(\mathbf{R}) \mathcal{U}_{p_i}^{*l_i}(\mathbf{R})$ —that is, the convolution of $\mathcal{U}_{p_s}^{*l_s}$ and $\mathcal{U}_{p_i}^{*l_i}$. Numerical calculations show that in the worst case—that is, $p_s = p_i$, $|l_s| = |l_i|$, and $R = 0$, for a 1-mm-thick crystal, pumped by a laser with $\lambda = 351$ nm and a waist of $w_0 = 1$ mm—the mean-square error is less than 1% for $N = 100$. Since we are neglecting the effects due to the anisotropy of the crystal, as discussed before, there is no point in seeking exact solutions for large values of N .

Under the thin-crystal approximation, Eq. (12) is more conveniently written in terms of Fourier transforms as

$$C_{p_s p_i}^{l_s l_i} \propto \int \int \int d\mathbf{R} d\mathbf{q} d\mathbf{q}' \mathcal{V}_p^l(\sqrt{2}\mathbf{q}') \mathcal{V}_{p_s}^{*l_s}(\mathbf{q}) \mathcal{V}_{p_i}^{*l_i}(\mathbf{q}) \times e^{i\mathbf{R} \cdot (\mathbf{q}' - \mathbf{q})} \propto \int d\mathbf{q} \mathcal{V}_p^l(\sqrt{2}\mathbf{q}) \mathcal{V}_{p_s}^{*l_s}(\mathbf{q}) \mathcal{V}_{p_i}^{*l_i}(\mathbf{q}), \quad (13)$$

where $\mathcal{V}_\mu^l(\mathbf{q})$ is the Fourier transform of $U_\mu^l(\mathbf{R})$. Writing Eq. (13) in cylindrical coordinates $\mathbf{q} \rightarrow (q, \phi)$, the LG profiles are $\mathcal{V}_\mu^l(\mathbf{q}) = v_\mu^l(q) e^{i\nu\phi}$. Then, we have

$$C_{p_s p_i}^{l_s l_i} \propto \int \int q dq d\phi v_p^l(\sqrt{2}q) v_{p_s}^{*l_s}(q) v_{p_i}^{*l_i}(q) e^{-i(l_s + l_i - l)\phi}, \quad (14)$$

that is,

$$C_{p_s p_i}^{l_s l_i} \propto \delta_{l_s + l_i, l} \int q dq v_p^l(\sqrt{2}q) v_{p_s}^{*l_s}(q) v_{p_i}^{*l_i}(q). \quad (15)$$

Thus, orbital angular momentum is conserved in the SPDC process. In principle, this conservation could be satisfied by fields exhibiting either a classical or quantum correlation (entanglement) of orbital angular momentum. We will now show that the conservation leads to entanglement of orbital angular momentum of the down-converted fields.

From Eq. (9) it is evident that, when $\mathcal{F}=1$, the biphoton wave function reproduces the pump beam transverse profile. Let us assume that Eq. (9) (with $\mathcal{F}=1$) accurately describes the two-photon state from SPDC and that the pump beam is a LG mode with $l \neq 0$. Then, the biphoton wave function is

$$\Psi(\boldsymbol{\rho}_s, \boldsymbol{\rho}_i) = \mathcal{U}_p^l \left(\frac{\boldsymbol{\rho}_s + \boldsymbol{\rho}_i}{\sqrt{2}} \right), \quad (16)$$

from which it is evident that $\Psi(\boldsymbol{\rho}_s + \boldsymbol{\Delta}, \boldsymbol{\rho}_i - \boldsymbol{\Delta}) = \Psi(\boldsymbol{\rho}_s, \boldsymbol{\rho}_i)$. Due to the phase structure of \mathcal{U}_p^l , for $l \neq 0$ there exist transverse spatial positions $\boldsymbol{\rho}_{s0}$ and $\boldsymbol{\rho}_{i0}$ such that $\mathcal{U}_p^l(\boldsymbol{\rho}_{s0} + \boldsymbol{\rho}_{i0}) = 0$. Then, clearly,

$$\Psi(\boldsymbol{\rho}_{s0} + \boldsymbol{\Delta}, \boldsymbol{\rho}_{i0} - \boldsymbol{\Delta}) = \Psi(\boldsymbol{\rho}_{s0}, \boldsymbol{\rho}_{i0}) = 0 \quad (17)$$

and the coincidence detection probability $\mathcal{P}(\boldsymbol{\rho}_s, \boldsymbol{\rho}_i) = |\Psi(\boldsymbol{\rho}_s, \boldsymbol{\rho}_i)|^2$ satisfies

$$\mathcal{P}(\boldsymbol{\rho}_{s0} + \boldsymbol{\Delta}, \boldsymbol{\rho}_{i0} - \boldsymbol{\Delta}) = \mathcal{P}(\boldsymbol{\rho}_{s0}, \boldsymbol{\rho}_{i0}) = 0. \quad (18)$$

Now suppose that the down-converted fields exhibit a classical correlation that conserves orbital angular momentum. The detection probability \mathcal{P}_{cc} for such a correlation can be written as

$$\mathcal{P}_{cc}(\boldsymbol{\rho}_s, \boldsymbol{\rho}_i) = \sum_{l_i=-\infty}^{\infty} P_{l_i} |F_{l-l_i}(\boldsymbol{\rho}_s)|^2 |G_{l_i}(\boldsymbol{\rho}_i)|^2, \quad (19)$$

where $F_{l_s}(\boldsymbol{\rho}_s)$ and $G_{l_i}(\boldsymbol{\rho}_i)$ represent down-converted signal and idler fields with orbital angular momentum $l_s \hbar$ and $l_i \hbar$

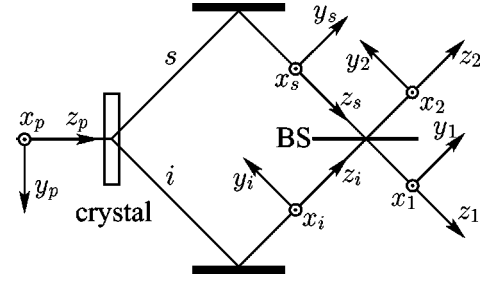


FIG. 1. The Hong-Ou-Mandel interferometer. Reflection at the beam splitter causes a sign change in the y coordinate.

per photon, respectively. Here the coefficients P_{l_i} satisfy $\sum_{l_i=-\infty}^{\infty} P_{l_i} = 1$ and $P_{l_i} \geq 0$. Now, if Eq. (19) accurately describes the two-photon state, then it must also satisfy the equivalent of Eq. (18):

$$\mathcal{P}_{cc}(\boldsymbol{\rho}_{s0} + \boldsymbol{\Delta}, \boldsymbol{\rho}_{i0} - \boldsymbol{\Delta}) = \mathcal{P}_{cc}(\boldsymbol{\rho}_{s0}, \boldsymbol{\rho}_{i0}) = 0,$$

which gives

$$\sum_{l_i=-\infty}^{\infty} P_{l_i} |F_{l-l_i}(\boldsymbol{\rho}_{s0} + \boldsymbol{\Delta})|^2 |G_{l_i}(\boldsymbol{\rho}_{i0} - \boldsymbol{\Delta})|^2 = 0. \quad (20)$$

Since $P_{l_i} \geq 0$, a nontrivial solution to Eq. (20) exists (for the cases where at least one $P_{l_i} \neq 0$) only if $|F_{l-l_i}(\boldsymbol{\rho}_{s0} + \boldsymbol{\Delta})|^2 = 0$ or $|G_{l_i}(\boldsymbol{\rho}_{i0} - \boldsymbol{\Delta})|^2 = 0$ for all $\boldsymbol{\Delta}$, which implies that $F_{l-l_i} \equiv 0$ or $G_{l_i} \equiv 0$. Thus, a classical correlation of orbital angular momentum states cannot reproduce the two photon wave function (9).

With the reasoning above, we have shown that, assuming Eq. (9) accurately describes the biphoton wave function from SPDC, the conservation of orbital angular momentum in SPDC is not satisfied by a classical correlation of the down-converted fields. This implies that the fields are entangled in orbital angular momentum.

B. Hong-Ou-Mandel interferometer

Having demonstrated that the two-photon wave function (7) leads to conservation and entanglement of orbital angular momentum, the next step is to prove that it describes accurately the state generated by SPDC within the assumed approximations. Although direct coincidence detection provides information about the modulus of $\Psi(\boldsymbol{\rho}_s, \boldsymbol{\rho}_i)$, its phase structure can only be revealed by some sort of interference measurement. We do this with the help of the Hong-Ou-Mandel (HOM) interferometer [12], represented in Fig. 1 and described below. Coincidence measurements are taken from the two output ports of the beam splitter. When the interferometer is balanced—that is, when paths s and i are equal—we have fourth-order interference. When the path length difference is much greater than the coherence length of the down-converted fields, the interferometer plays essentially no role other than decreasing the coincidence counts by a factor of 1/2, and we can perform simple coincidence measurements.

In the HOM interferometer, the state (3) is incident on a symmetric beam splitter as shown in Fig. 1. The annihilation operators in modes 1 and 2 after the beam splitter can be expressed in terms of the operators in modes s and i :

$$\mathbf{a}_1(\mathbf{q}) = t\mathbf{a}_s(q_x, q_y) + ir\mathbf{a}_i(q_x, -q_y), \quad (21)$$

$$\mathbf{a}_2(\mathbf{q}) = t\mathbf{a}_i(q_x, q_y) + ir\mathbf{a}_s(q_x, -q_y), \quad (22)$$

where t and r are the transmission and reflection coefficients of the beam splitter. The negative sign that appears in q_y components is due to the reflection from the beam splitter, as shown in Fig. 1. If \mathbf{r}_1 and \mathbf{r}_2 are the positions of detectors D_1 and D_2 , each located at one output of the beam splitter, the coincidence detection amplitude is given by

$$\Psi_c = \Psi_{tt}(\mathbf{r}_1, \mathbf{r}_2) + \Psi_{rr}(\mathbf{r}_1, \mathbf{r}_2), \quad (23)$$

where the indices tt and rr refer to the cases when both photons are transmitted or reflected by the beam splitter, respectively. Combining Eq. (9) with $\mathcal{F} \equiv 1$ and Eqs. (21)–(23), it is straightforward to show that, for $t=r=1/\sqrt{2}$, apart from a common factor,

$$\Psi_c(\boldsymbol{\rho}_1, \boldsymbol{\rho}_2) \propto \frac{1}{2} \left[\mathcal{U} \left(\frac{x_1 + x_2}{\sqrt{2}}, \frac{y_1 + y_2}{\sqrt{2}} \right) - \mathcal{U} \left(\frac{x_1 + x_2}{\sqrt{2}}, \frac{-y_1 - y_2}{\sqrt{2}} \right) \right]. \quad (24)$$

Since the pump beam is a LG beam, \mathcal{U} has the form

$$\mathcal{U}(\boldsymbol{\rho}) = u_p^l(\rho) e^{il\phi}. \quad (25)$$

According to Eq. (24), the corresponding coincidence detection amplitude is

$$\Psi_c(\boldsymbol{\rho}_1, \boldsymbol{\rho}_2) = \Psi_c(R, \theta) \propto u_p^l(R) \sin l\theta, \quad (26)$$

where $R = (1/\sqrt{2})|\boldsymbol{\rho}_1 + \boldsymbol{\rho}_2|$ and θ is defined by the relations

$$\sin \theta = \frac{\rho_1 \sin \phi_1 + \rho_2 \sin \phi_2}{R}, \quad (27)$$

$$\cos \theta = \frac{\rho_1 \cos \phi_1 + \rho_2 \cos \phi_2}{R}. \quad (28)$$

The coincidence detection probability, which is proportional to $|\Psi_c(R, \theta)|^2$, is

$$P_{12}(\boldsymbol{\rho}_1, \boldsymbol{\rho}_2) \propto |u_p^l(R)|^2 \sin^2 l\theta. \quad (29)$$

III. EXPERIMENT

The experimental setup, shown in Fig. 2, consists of two basic parts. The first part is the generation of a Laguerre-Gaussian mode using a mode converter, which transforms a Hermite-Gaussian mode into a LG mode. A detailed account of mode conversion can be found in Refs. [13,14]. To create the HG mode, we insert a 25- μm -diam wire into the cavity

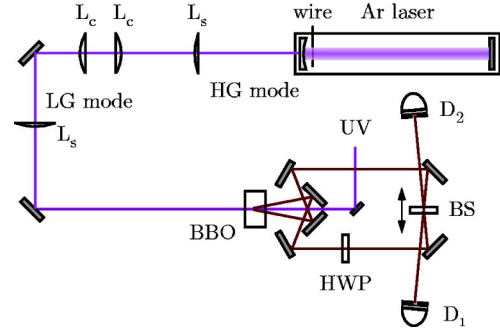


FIG. 2. Experimental setup. A wire is inserted into the laser cavity in order to generate a HG mode. A mode converter consisting of two identical spherical (L_s) and cylindrical (L_c) lenses converts the HG mode to a LG mode of the same order. The LG mode is then used to pump the BBO crystal, generating entangled photons incident on a HOM interferometer. The beam splitter BS is mounted on a motorized stage. Coincidence counts are recorded at detectors D_1 and D_2 .

of an argon laser, operating at ~ 30 mW with wavelength 351.1 nm. The wire breaks the circular symmetry of the laser cavity. It is aligned in the horizontal or vertical and mounted on an xy -translation stage. By adjusting the position and orientation of the wire, we can generate the modes HG_{01} , HG_{10} , HG_{02} , and HG_{20} . The beam then passes through a mode converter consisting of two spherical lenses (L_s) with focal length $f_s = 500$ mm and two cylindrical lenses (L_c) with focal length $f_c = 50.2$ mm. The first spherical lens is used for mode matching and is located ≈ 1.88 m from the beam center of curvature. The second spherical lens is placed confocal with the first and is used to “collimate” the beam. The cylindrical lenses are placed ($d = f_c/\sqrt{2} \approx 35$ mm) on either side of the focal point of lens L_s and aligned at 45° . The cylindrical lenses transform the HG mode into a LG mode of the same order by introducing a relative $\pi/2$ phase between successive HG components (in the $\pm 45^\circ$ basis, due to the orientation of the cylindrical lenses) of the input beam [13,14]. The quality of the output mode was checked by visual examination of the intensity profile [15] as well as by interference techniques: using additional beam splitters and mirrors (not shown), the interference of the LG pump beam with a plane wave resulted in the usual spiral interference pattern [14].

The second part of the setup is a typical HOM interferometer [12]. The argon laser is used to pump a 7-mm-long BBO ($\beta\text{-BaB}_2\text{O}_4$) crystal cut for type-II phase matching, generating noncollinear entangled photons by SPDC. The down-converted photons are reflected through a system of mirrors and incident on a beam splitter with measured transmittance $T \approx 0.67$ and reflectance $R \approx 0.33$. Since the down-converted photons are orthogonally polarized, a half-wave plate (HWP) is used to rotate the polarization of one of the photons ($V \rightarrow H$). A computer-controlled stepper motor is used to adjust the position of the beam splitter. The detectors are EG&G SPCM 200 photodetectors, mounted on precision translation stages. D_2 remained fixed while a computer-controlled stepper motors were used to scan detector D_1 in the transverse plane. Coincidence and single counts were

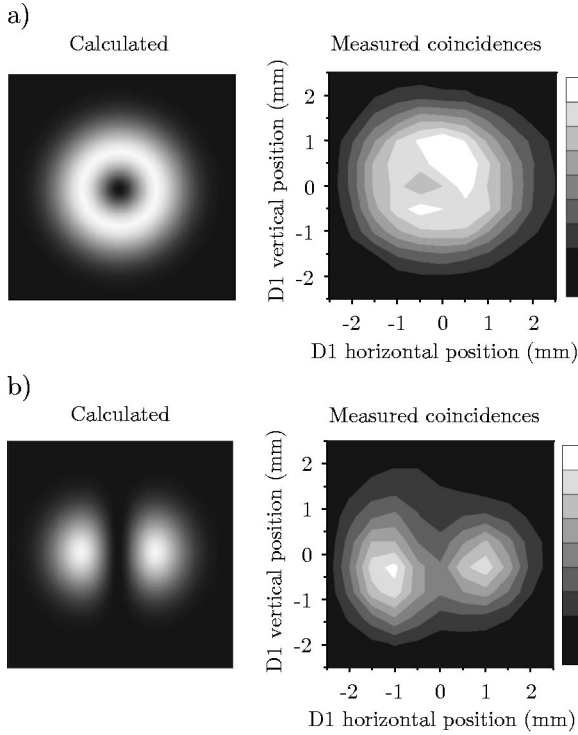


FIG. 3. Coincidence profiles predicted (left) and measured (right) when the crystal is pumped by a LG_0^1 beam. (a) No-interference regime (Hong-Ou-Mandel interferometer unbalanced). (b) Fourth-order interference regime (interferometer balanced).

registered using a personal computer. Interference filters [1 nm full width at half maximum (FWHM) centered at 702 nm] and 2-mm circular apertures were used to align the HOM interferometer. The transverse intensity profiles were measured with the interference filters removed and circular apertures with diameter 0.5 mm and 1 mm on D_1 and D_2 , respectively.

IV. RESULTS AND DISCUSSION

The results are shown in Figs. 3–5. The left sides of the figures show the expected coincidence patterns, obtained from the squared modulus of Eq. (9) in the noninterfering regime (interferometer unbalanced) and from Eq. (29) in the fourth-order interference regime (interferometer balanced). The right sides of the figures show the measured coincidences.

In Fig. 3, the nonlinear crystal was pumped by a LG_0^1 ($l = 1$) beam. Its intensity profile is shown in Fig. 3(a), in agreement with Eq. (9). In the interference regime, shown in Fig. 3(b), the two interference peaks predicted by Eq. (29) are easily seen. In Fig. 4, the nonlinear crystal was pumped by a LG_0^2 ($l = 2$) beam. Now, the interference pattern shows four peaks, in agreement with Eq. (29).

In order to test the translational invariance of $\Psi(\rho_1, \rho_2)$, which leads to the conclusion that the two-photon state is entangled in orbital angular momentum, we repeated the measurement of Fig. 3(b), with detector D_2 displaced by $\Delta x = \Delta y = 1$ mm. The interference pattern obtained is shown

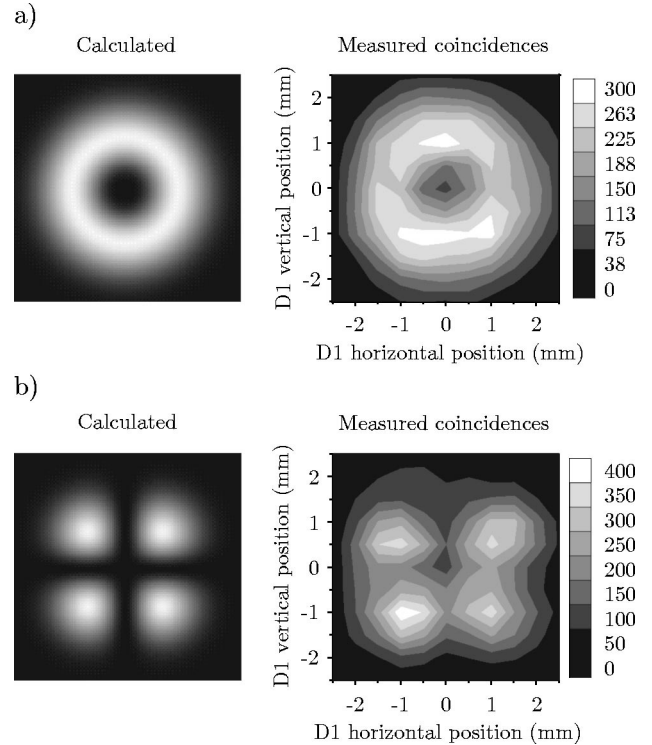


FIG. 4. Coincidence profiles predicted (left) and measured (right) when the crystal is pumped by a LG_0^2 beam. (a) No-interference regime (Hong-Ou-Mandel interferometer unbalanced). (b) Fourth-order interference regime (interferometer balanced).

in Fig. 5. The coincidence pattern measured by scanning D_1 is now dislocated by $\Delta x = \Delta y = -1$ mm, still in agreement with Eq. (29).

V. CONCLUSION

We have shown experimentally that our theoretical description of the two-photon wave function is accurate. Information about its modulus and phase structure was obtained by direct coincidence detection and coincidence detection of fourth-order HOM interference effects, respectively. The transfer of the plane-wave spectrum of the pump beam to the fourth-order transverse spatial correlation function of the

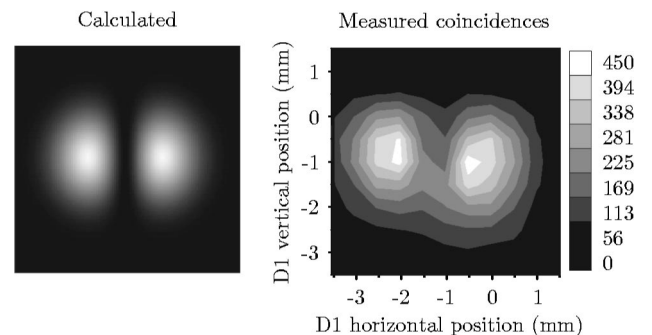


FIG. 5. Coincidence profile predicted (left) and measured (right) when the crystal is pumped by a LG_0^1 beam, in the fourth-order interference regime (Hong-Ou-Mandel interferometer balanced). Detector D_2 was displaced by $\Delta x = \Delta y = 1$ mm.

two-photon field generated by SPDC leads to the conservation and entanglement of the orbital angular momentum of the down-converted fields. We should stress that this effect is restricted to the context of two approximations. The first is the paraxial approximation, in which our model for the transfer of the plane-wave spectrum in SPDC is based. However, the paraxial approximation is also the context in which the angular momentum carried by electromagnetic beams can be separated into an intrinsic part, associated with polarization, and an orbital part, associated with the transverse phase structure of the beam. The second approximation is the so-called thin-crystal approximation. It is possible to show that this approximation would not be necessary if the nonlinear medium were isotropic. The birefringence of the crystals

used for SPDC causes nonconservation of the orbital angular momentum that is proportional to the crystal length. Rigorously speaking, orbital angular momentum would never be conserved in SPDC due to this effect. In thin crystals (a few millimeters in length), however, it can be neglected. We believe that the arguments and experiment reported here provide additional evidence of conservation and entanglement of the orbital angular momentum of light in SPDC, as well as the limits within which they should be understood.

ACKNOWLEDGMENTS

The authors thank the Brazilian funding agencies CNPq and CAPES.

-
- [1] L. Allen, M.W. Beijersbergen, R.J.C. Spreeuw, and J.P. Woerdman, *Phys. Rev. A* **45**, 8185 (2002).
 - [2] H.H. Arnaut and G.A. Barbosa, *Phys. Rev. Lett.* **85**, 286 (2000).
 - [3] E.R. Eliel, S.M. Dutra, G. Nienhuis, and J.P. Woerdman, *Phys. Rev. Lett.* **86**, 5208 (2001).
 - [4] J. Leach, M. Padgett, S.M. Barnett, S. Franke-Arnold, and J. Courtial, *Phys. Rev. Lett.* **88**, 257901 (2002).
 - [5] A. Mair, A. Vaziri, G. Weihs, and A. Zeilinger, *Nature (London)* **442**, 313 (2001).
 - [6] S. Franke-Arnold, S.M. Barnett, M.J. Padgett, and L. Allen, *Phys. Rev. A* **65**, 033823 (2002).
 - [7] G.A. Barbosa and H.H. Arnaut, *Phys. Rev. A* **65**, 053801 (2002).
 - [8] J.P. Torres, Y. Deyanova, L. Torner, and G. Molina-Terriza, *Phys. Rev. A* **67**, 052313 (2003).
 - [9] C.H. Monken, P.H.S. Ribeiro, and S. Pádua, *Phys. Rev. A* **57**, 3123 (1998).
 - [10] C.K. Hong and L. Mandel, *Phys. Rev. A* **31**, 2409 (1985).
 - [11] P.G. Kwiat, K. Mattle, H. Weinfurter, A. Zeilinger, A.V. Sergienko, and Y. Shih, *Phys. Rev. Lett.* **75**, 4337 (1995).
 - [12] C.K. Hong, Z.Y. Ou, and L. Mandel, *Phys. Rev. Lett.* **59**, 2044 (1987).
 - [13] M.W. Beijersbergen, L. Allen, H.E.L.O. van der Veen, and J.P. Woerdman, *Opt. Commun.* **96**, 123 (1993).
 - [14] M. Padgett, J. Arlt, N. Simpson, and L. Allen, *Am. J. Phys.* **64**, 77 (1996).
 - [15] J. Courtial and M. Padgett, *Opt. Commun.* **159**, 13 (1999).